

See discussions, stats, and author profiles for this publication at: <https://www.researchgate.net/publication/224935506>

Computational study of bonding trends in the metalloactinyl series EThM and MThM' (E = N-, O, F+; M, M' = Ir-, Pt, Au+)

ARTICLE *in* CHEMICAL PHYSICS LETTERS · NOVEMBER 2006

Impact Factor: 1.9 · DOI: 10.1016/j.cplett.2006.08.144

CITATIONS

8

READS

20

3 AUTHORS:



[Peter Hrobárik](#)

Technische Universität Berlin

35 PUBLICATIONS 582 CITATIONS

SEE PROFILE



[Michal Straka](#)

Academy of Sciences of the Czech Republic

62 PUBLICATIONS 1,020 CITATIONS

SEE PROFILE



[Pekka Pyykkö](#)

University of Helsinki

325 PUBLICATIONS 14,349 CITATIONS

SEE PROFILE

Computational study of bonding trends in the metalloactinyl series EThM and MThM' (E = N⁻, O, F⁺; M, M' = Ir⁻, Pt, Au⁺)

Peter Hrobárik^{a,b}, Michal Straka^b, Pekka Pyykkö^{b,*}

^a Institute of Inorganic Chemistry, Slovak Academy of Sciences, Dúbravská cesta 9, SK-84536 Bratislava, Slovakia

^b Department of Chemistry, University of Helsinki, P.O. Box 55 (A. I. Virtasen aukio 1), FIN-00014 Helsinki, Finland

Received 30 June 2006; in final form 3 August 2006

Available online 19 September 2006

Abstract

The title systems, including EThE', are treated at DFT level using a B3LYP functional and small-core quasirelativistic pseudopotentials. Most of the studied systems are bent, like their isoelectronic ThO₂ analogue, except for some anionic systems containing Ir. The bond lengths vary considerably and can lie above or below the sum of triple-bond covalent radii. Among the studied systems, the iridium-containing species show the strongest back-donation to Th. The bonding can be simply understood and could theoretically go up to a '24-electron principle' limit at the actinide.

© 2006 Elsevier B.V. All rights reserved.

1. Introduction

A chemical analogy between oxygen and platinum (or Au⁺) was discovered by Pyykkö et al. [1] for multiply-bonded molecular systems, with the O/Pt at the end of a chemical bond. Similar analogies, such as N/Ir, apply for the neighbouring transition metals. A simple pictorial explanation can be given to this analogy [2] and this reasoning was found helpful in developing a set of triple-bond covalent radii for the elements Be–E112 [3].

The same idea was applied to replacing main-group atoms in uranyl UO₂²⁺ or isoelectronic systems by Gagliardi and Pyykkö [4], who also found well-developed triple bonds at both ends, E≡U and U≡M(nd). The first member of the predicted series, OUIr⁺, was already experimentally produced in the gas-phase [7]. This species is analogous to the known OUN⁺, Ir replacing N. The related OUAu⁺ and OUPt⁺ as well as other triatomics were also mass-spectroscopically observed. Furthermore

UIr⁺, UPt⁺ and UAu⁺ and other diatomics were found [7], see also [8,9]. Large dissociation energies were reported for some of them.

A good name for this triatomic series would be *metalloactinyls*. We also repeat the point about *autogenic isolobality* [1]: In the usual isolobal picture an –ML_n group mimics the chemical behaviour of a –CH_m group. Here the –M metal atom at the end of a bond does the same thing without help of any ligands, L.

More generally speaking, the actinide-transition metal An–M(nd) bonds in bulk compounds still remain rather unexplored. The Cp₃AnM(Cp)(CO)₂ (An = Th, U; M = Fe, Ru) were synthesized ([10] and references cited therein) and contained unbridged (ligand unsupported) An–M(nd) bonds. Furthermore, the phosphido-bridged Th–Ni bond in Cp₂Th(μ-PPh₂)₂Ni(CO)₂, and the Th–Pt bond in an analogous complex where two CO ligands are replaced by PMe₃, were prepared [11,12]. Theoretical calculations suggested a normal σ bond between Th and Pt. While multiple bonds between two transition metals are well known (for instance the triple or quadruple bonds in dirhenium and dimolybdenum compounds) and theoretically studied by many authors, only little attention has

* Corresponding author. Fax: +358 9 191 50169.

E-mail addresses: peter.hrobarik@savba.sk (P. Hrobárik), pekka.pyykkko@helsinki.fi (P. Pyykkö).

been devoted to understanding the chemical bonding between an actinide and a transition metal or even two actinide atoms. [13,14].

The isoelectronic thinking mentioned above suggests an entire family of metalloactinyls, where one or both main-group elements are replaced by transition metals. Here we report the results of a study of a metalloactinyl and bimetalloactinyl series, where the actinide atom is thorium and the transition metal atoms are Ir[−], Pt or Au⁺. The bonding trends are discussed in comparison to the corresponding Th-main group element actinyls. It is interesting to see what changes, if any, would occur when passing from the normal actinyls to metalloactinyls.

As well known, ThO₂ is a bent C_{2v} system [15,16], while UO₂²⁺ is linear [17]. The computationally characterized PaO₂⁺ and NpO₂³⁺ are also linear [18–20]. This presumably general behavior was explained intuitively by an increasing 5f character, compared with the relatively constant 6d character along the Th–Pu series [18,21].

2. Methods

The calculations were performed with the GAUSSIAN 03 program package [22] at the B3LYP density functional level of theory. The convergence criterion *scf* = *tight* and the integration grid option *grid* = *ultrafine* were used to ensure a good numerical accuracy. For both Th and the 5d metals, energy-adjusted relativistic small-core Stuttgart

pseudopotentials (60 core electrons for Th) [23,24] were employed. The corresponding GTO valence basis sets were of quality (8s 7p 6d)/[6s 5p 3d] for Ir, Pt, Au and (12s 11s 10d 8f)/[8s 7p 6d 4f] for Th. Two g functions with exponents $\alpha_1 = 1.524$, $\alpha_2 = 0.375$ [18] were added to the basis set of thorium, and one polarization f function to the basis set of 5d metals (corresponding exponents: $\alpha = 0.967$ for Ir, $\alpha = 0.986$ for Pt, $\alpha = 1.056$ for Au) [25].

The relativistic small-core (60 electrons) pseudopotentials and basis set of the same quality as for Th were used for Pa atom (two g functions with the same exponents were employed).

A TZVP all-electron basis was used on main-group atoms [26]. In the earlier work [4], it was shown that the inclusion of spin–orbit coupling on the structure of the isoelectronic NUir molecule in its ground state is not important. Therefore spin–orbit coupling is expected to be of minor importance for most of the structures studied here, particularly for those ones, which are closed-shell singlets in ground states. We also expect that neither the exchange–correlation functional nor basis set or integration accuracy would strongly affect the trends to be discussed. The hybrid DFT methods, pseudopotentials, and basis sets used in this work have been shown to provide rather accurate structures and energies for both transition metal and actinide systems. The bonding was studied by means of Natural Bond Orbital (NBO), Natural Localized Molecular Orbitals (NLMO) and Natural Population Analyses

Table 1
Geometry parameters and relative energies of the E–Th–E' species; E, E' = N[−], O, F⁺

E–Th–E'	Symmetry	State	<i>R</i> _{Th–E} (pm)	<i>R</i> _{Th–E'} (pm)	∠ _{EThE'} (degree)	Δ <i>E</i> (kJ mol ^{−1})	<i>N</i>	μ (D)
FThF ²⁺	D _{∞h}	¹ Σ _g	196.2	196.2	180.0	23.6	1	0.00
		³ Σ _g	209.6	209.6	180.0	634.2	1	0.00
	C _{2v}	¹ A ₁	195.5	195.5	110.3	0.0	0	4.94
		³ B ₂	218.9	218.9	54.4	596.4	0	6.18
FThO ⁺	C _{∞v}	¹ Σ	206.7	181.7	180.0	29.4	1	1.43
		³ Σ	201.2	197.2	180.0	367.7	0	0.45
	C _s	¹ A'	204.9	182.2	115.2	0.0	0	5.92
		³ A'	200.4	209.8	106.3	365.3	0	4.25
FThN	C _{∞v}	¹ Σ	220.7	180.9	180.0	36.9	1	3.53
		³ Σ	211.7	192.0	180.0	91.4	1	1.28
	C _s	¹ A'	215.0	182.2	116.6	0.0	0	7.25
		³ A'	210.0	192.4	121.5	79.6	0	3.30
OThO	D _{∞h}	¹ Σ _g	189.6	189.6	180.0	40.6	1	0.00
		³ Σ _g	191.7	191.7	180.0	225.1	0	0.00
	C _{2v}	¹ A ₁	189.9	189.9	119.1	0.0	0	6.77
		³ B ₂	209.1	209.1	42.0	526.0	0	5.07
OThN [−]	C _{∞v}	¹ Σ	200.2	187.8	180.0	45.6	1	2.00
		³ Σ	194.0	197.9	180.0	118.5	1	0.02
	C _s	¹ A'	197.8	190.3	119.5	13.4	0	7.73
		³ A'	193.5	200.0	123.5	0.0	0	2.86
NThN ^{2−}	D _{∞h}	¹ Σ _g	192.7	192.7	180.0	37.7	2	0.00
		³ Σ _g	194.6	194.6	180.0	24.8	1	0.00
	C _{2v}	¹ A ₁	193.1	193.1	154.2	35.6	0	0.36
		³ B ₂	196.3	196.3	125.0	0.0	0	4.38

Number of imaginary frequencies *N* and dipole moments *μ* are also given.

(NPA) [5,6], using the built-in NBO-3.1 subroutines of the GAUSSIAN 03 program.

Dipole moments were also evaluated as criteria for structure elucidation. In the case of neutral molecules, the dipole moment is independent on the location of the origin. For charged species the origin is the centre-of-nuclear-charge.

3. Results and discussion

3.1. Structures

The calculated structures and their relative energies are shown in Tables 1–3. The species PtThIr[−] and NThIr^{2−} are found to be singlet-state linear structures while NThPt[−] and OThIr[−] are border-line cases. IrThIr^{2−} is expected to have a linear triplet ground state. These systems extend

the series of uranium-containing linear singlet species in ref. [4]. Note that PtThIr[−] contains three heavy metals and no main-group elements. The border-line cases have very flat-bottom bending potentials.

All the other species are bent singlets, except OThN[−] and NThN^{2−} which have a bent triplet ground state. As shown in Fig. 1, the inversion barriers can be quite low. The mechanisms behind the bending have been discussed before, see [19,21] and references there. The fact that ThO₂ has a larger energetic barrier than the analogous ThPt₂, can be understood from NPA analysis (see Table 4): When one tries to straighten ThO₂, the ligand 2p electrons can only overlap with the higher-lying f orbitals, while in ThPt₂ the ligand atoms still have available d orbitals. The linear ThO₂ would have a high f population.

The bond lengths reveal some interesting trends and new aspects. In the previous study of uranium metalloactinyls

Table 2
Geometry parameters and relative energies of the E–Th–M species; E = N[−], O, F⁺, M = Ir[−], Pt, Au⁺

E–Th–M	Symmetry	State	$R_{\text{Th–E}}$ (pm)	$R_{\text{Th–M}}$ (pm)	\angle_{MThM} (degree)	ΔE (kJ mol ^{−1})	N	μ (D)
FThAu ²⁺	$C_{\infty v}$	¹ Σ	195.5	264.2	180.0	45.1	1	5.80
		³ Σ	196.4	314.7	180.0	203.4	1	3.75
	C_s	¹ A'	195.3	261.7	104.1	0.0	0	8.33
		³ A'	198.0	310.5	90.9	169.7	0	6.90
OThAu ⁺	$C_{\infty v}$	¹ Σ	180.8	275.7	180.0	31.0	1	2.24
		³ Σ	181.9	324.2	180.0	239.8	1	1.08
	C_s	¹ A'	181.4	273.0	113.3	0.0	0	6.97
		³ A'	182.4	313.5	74.0	233.3	0	5.75
NThAu	$C_{\infty v}$	¹ Σ	180.1	290.0	180.0	13.3	1	2.53
		³ Σ	190.0	285.8	180.0	129.4	1	0.77
	C_s	¹ A'	180.8	286.6	125.6	0.0	0	6.17
		³ A'	190.9	283.8	132.8	125.9	0	2.48
FThPt ⁺	$C_{\infty v}$	¹ Σ	202.6	235.9	180.0	36.8	1	3.83
		³ Σ	202.4	245.3	180.0	205.8	1	0.76
	C_s	¹ A'	202.5	235.0	113.8	0.0	0	6.27
		³ A'	202.3	253.0	105.5	185.0	0	4.46
OThPt	$C_{\infty v}$	¹ Σ	185.9	243.7	180.0	13.4	1	0.59
		³ Σ	187.0	246.3	180.0	187.1	0	1.92
	C_s	¹ A'	186.8	244.4	127.1	0.0	0	5.15
		³ A'	186.2	268.0	113.3	187.7	0	3.58
NThPt [−]	$C_{\infty v}$	¹ Σ	184.8	252.9	180.0	0.1	1	3.89
		³ Σ	193.8	249.2	180.0	92.6	1	2.35
	C_s	¹ A'	184.8	252.9	173.8	0.0	0	3.95
		³ A'	195.0	249.7	135.8	81.6	0	2.68
FThIr	$C_{\infty v}$	¹ Σ	211.1	224.6	180.0	22.7	1	2.66
		³ Σ	209.4	222.9	180.0	136.3	0	0.19
	C_s	¹ A'	211.3	225.4	121.7	0.0	0	4.61
		³ A'	208.0	243.2	112.2	108.3	0	3.24
OThIr [−]	$C_{\infty v}$	¹ Σ	192.1	229.5	180.0	0.1	0	0.26
		³ Σ	191.8	227.8	180.0	96.0	1	2.42
	C_s	¹ A'	192.3	230.0	161.4	0.0	0	1.77
		³ A'	190.6	252.6	118.2	59.6	0	2.74
NThIr ^{2−}	$C_{\infty v}$	¹ Σ	190.3	231.1	180.0	0.0	0	8.32
		³ Σ	191.5	230.5	180.0	17.1	0	13.70
	C_s	¹ A'	minima not found \Rightarrow linear					
		³ A'	minima not found \Rightarrow linear					

Number of imaginary frequencies N and dipole moments μ are also given.

Table 3

Geometry parameters and relative energies of the M–Th–M' species; M, M' = Ir[−], Pt, Au⁺

M–Th–M'	Symmetry	State	$R_{\text{Th–M}}$ (pm)	$R_{\text{Th–M'}}$ (pm)	$\angle_{\text{MThM'}}$ (degree)	ΔE (kJ mol ^{−1})	N	μ (D)
AuThAu ²⁺	$D_{\infty h}$	$^1\Sigma_g$	262.7	262.7	180.0	64.8	1	0.00
		$^3\Sigma_g$	274.7	274.7	180.0	188.1	1	0.00
	C_{2v}	1A_1	261.6	261.6	106.3	0.0	0	7.03
		3B_2	282.0	282.0	60.8	110.9	0	8.79
AuThPt ⁺	$C_{\infty v}$	$^1\Sigma$	271.8	234.7	180.0	42.4	1	0.51
		$^3\Sigma$	279.0	236.9	180.0	224.7	1	0.86
	C_s	$^1A'$	270.9	235.0	115.0	0.0	0	5.91
		$^3A'$	284.5	243.5	65.1	136.8	0	6.46
AuThIr	$C_{\infty v}$	$^1\Sigma$	285.9	224.0	180.0	18.7	1	1.63
		$^3\Sigma$	284.8	223.3	180.0	126.7	0	0.10
	C_s	$^1A'$	284.4	224.1	125.6	0.0	0	4.70
		$^3A'$	281.5	241.7	115.4	126.6	0	3.19
PtThPt	$D_{\infty h}$	$^1\Sigma_g$	240.5	240.5	180.0	11.8	1	0.00
		$^3\Sigma_g$	242.6	242.6	180.0	150.1	0	0.00
	C_{2v}	1A_1	241.1	241.1	132.7	0.0	0	4.76
		3B_2	247.5	247.5	71.7	145.9	0	4.23
PtThIr [−]	$C_{\infty v}$	$^1\Sigma$	248.3	227.6	180.0	0.0	0	1.58
		$^3\Sigma$	248.9	227.2	180.0	118.5	1	0.02
	C_s	$^1A'$	minima not found \Rightarrow linear					
		$^3A'$	248.1	227.0	153.8	114.5	0	1.59
IrThIr ^{2−}	$D_{\infty h}$	$^1\Sigma_g$	231.2	231.2	180.0	8.3	0	0.00
		$^3\Sigma_g$	228.3	228.3	180.0	0.0	0	0.00
	C_{2v}	1A_1	minima not found \Rightarrow linear					
		3B_2	minima not found \Rightarrow linear					

Number of imaginary frequencies N and dipole moments μ are also given.

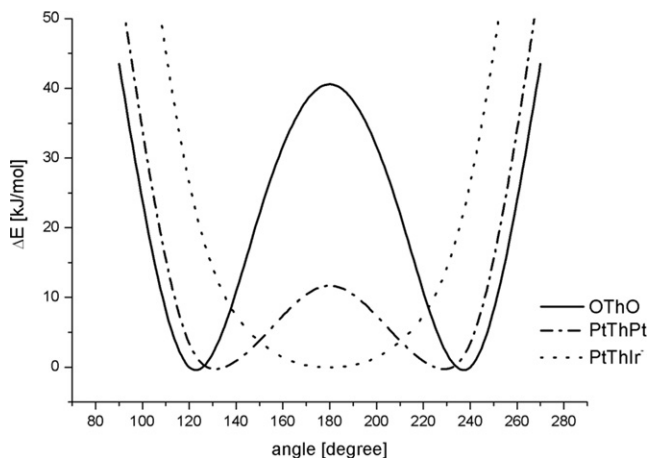


Fig. 1. The calculated bending potential curve for ThO₂ and for the bimetalloactinyls ThPt₂ and PtThIr[−].

[4], both two bonds were found to be localized $\sigma^2\pi^4$ triple bonds. NUIr was, in fact, used for developing the triple-bond covalent radii [3]. We now find preliminary indications that the M–An bonding can be even shorter than what is predicted by that rough device, as seen in Table 5. The shortest An–M bonds occur for the ground states of FThIr (225.4 pm), AuThIr (Th–Ir 224.1 pm) or PtThIr[−] (Th–Ir 227.6 pm). The three calculated $R(\text{Th–Ir})$ are clearly below the values, predicted by the sum of the triple-bond covalent radii.

The dipole moments in Table 1 are quite large, up to 6–7 D for the neutral molecules, which also suggests considerable charge transfer and polarization.

3.2. Bonding

The NPA charges are shown in Table 4. For PtThIr[−] they show a larger electron charge on Ir than on Pt. Pictures of the localized valence orbitals are shown in Fig. 2–4. A compact cartoon description of the bonding, of the type used previously [2,3], is shown in Fig. 5. A closer inspection of the bonding orbitals reveals, in addition to the previous localized σ and π bonds, a possible weak δ bond and an outer σ bond, having constructive interference between the diffuse ‘doughnut’ s–d hybrid orbitals on Ir and Th, see Figs. 3,4. The Th–Ir δ bond is self-explanatory. The outer σ bonds are shown in Fig. 4 at a lower density limit. The two σ bonds form a ‘sausage inside a tube’.

Before stronger claims are made, the question of higher bond-orders (than three) must be studied carefully, combining several methods. That lies outside the present first mapping. In the scheme of Fig. 5 we have 24 electrons, of which 20 can in principle bond, giving an upper limit of 6 for the Th–Ir bond-order.

As recently discussed [27] in context of the 18-electron principle and its possible extensions, thorocene, Th(C₈H₈)₂, effectively has 20e around its Th. This is the same number

Table 4
Calculated NPA charges Q and natural atomic populations for singlet states

System	Symmetry	Valence populations on Th					NPA charges		
		7s	7p	6d	5f	6p	Q_{Th}	Q_{M}	$Q_{\text{M}'}$
AuThAu ²⁺	D _{∞h}	0.45	0.00	0.40	0.58	5.98	2.52	−0.26	−0.26
	C _{2v}	0.61	0.00	0.75	0.30	5.97	2.35	−0.18	−0.18
AuThPt ⁺	C _{∞v}	0.54	0.00	0.58	0.61	5.97	2.29	−0.49	−0.80
	C _s	0.66	0.00	0.79	0.45	5.96	2.12	−0.41	−0.71
AuThIr	C _{∞v}	0.65	0.00	0.82	0.62	5.96	1.91	−0.68	−1.23
	C _s	0.74	0.00	0.97	0.53	5.95	1.77	−0.63	−1.15
PtThPt	D _{∞h}	0.56	0.00	0.65	0.75	5.97	2.06	−1.03	−1.03
	C _{2v}	0.63	0.00	0.81	0.62	5.96	1.95	−0.98	−0.98
PtThIr [−]	C _{∞v}	0.62	0.00	0.82	0.81	5.96	1.78	−1.27	−1.51
	C _s	minima not found							
IrThIr ^{2−}	D _{∞h}	0.61	0.00	0.88	0.94	5.94	1.61	−1.80	−1.80
	C _{2v}	minima not found							
FThAu ²⁺	C _{∞v}	0.31	0.01	0.28	0.58	5.96	2.84	−0.64	−0.20
	C _s	0.36	0.00	0.51	0.32	5.96	2.83	−0.66	−0.16
OThAu ⁺	C _{∞v}	0.34	0.02	0.44	0.64	5.91	2.63	−1.15	−0.48
	C _s	0.31	0.04	0.64	0.45	5.92	2.62	−1.19	−0.42
NThAu	C _{∞v}	0.55	0.04	0.77	0.52	5.88	2.23	−1.52	−0.71
	C _s	0.35	0.10	0.95	0.44	5.90	2.25	−1.60	−0.64
FThPt ⁺	C _{∞v}	0.48	0.00	0.42	0.70	5.95	2.43	−0.71	−0.72
	C _s	0.47	0.01	0.63	0.48	5.95	2.43	−0.73	−0.71
OThPt	C _{∞v}	0.49	0.01	0.50	0.83	5.90	2.25	−1.24	−1.01
	C _s	0.43	0.03	0.70	0.63	5.92	2.27	−1.28	−0.99
NThPt [−]	C _{∞v}	0.76	0.01	0.70	0.75	5.86	1.88	−1.59	−1.29
	C _s	0.76	0.02	0.70	0.74	5.87	1.88	−1.59	−1.29
FThIr	C _{∞v}	0.65	0.00	0.63	0.80	5.94	1.96	−0.79	−1.17
	C _s	0.63	0.01	0.82	0.60	5.94	1.94	−0.79	−1.15
OThIr [−]	C _{∞v}	0.60	0.01	0.62	0.97	5.89	1.86	−1.34	−1.52
	C _s	0.59	0.01	0.67	0.93	5.90	1.85	−1.34	−1.51
NThIr ^{2−}	C _{∞v}	1.09	0.01	0.72	0.94	5.82	1.27	−1.62	−1.66
	C _s	minima not found							
FThF ²⁺	D _{∞h}	0.01	0.00	0.23	0.57	5.94	3.24	−0.62	−0.62
	C _{2v}	0.01	0.02	0.35	0.37	5.95	3.29	−0.64	−0.64
FThO ⁺	C _{∞v}	0.05	0.00	0.36	0.80	5.89	2.88	−0.74	−1.14
	C _s	0.03	0.05	0.54	0.51	5.92	2.93	−0.74	−1.19
FThN	C _{∞v}	0.37	0.01	0.63	0.76	5.87	2.35	−0.87	−1.49
	C _s	0.11	0.13	0.88	0.50	5.89	2.47	−0.82	−1.65
OThO	D _{∞h}	0.09	0.02	0.39	1.12	5.83	2.53	−1.26	−1.26
	C _{2v}	0.04	0.08	0.68	0.66	5.88	2.63	−1.32	−1.32
OThN [−]	C _{∞v}	0.71	0.04	0.50	1.04	5.79	1.91	−1.46	−1.44
	C _s	0.19	0.16	0.92	0.66	5.86	2.16	−1.44	−1.72
NThN ^{2−}	D _{∞h}	1.91	0.02	0.43	0.80	5.61	0.91	−1.46	−1.46
	C _{2v}	1.89	0.03	0.64	0.70	5.64	0.98	−1.49	−1.49

as we find here for PtThIr[−]. If also the left-hand δ -ring would interact with Th, a case possible for IrThIr^{2−}, we would have the first example on a system following a ‘24-electron principle’. Only the ϕ -ring and the extra π of Th would then remain empty.

Concerning the possible hole in the 6p semicore shell, the EThE' species show values of up to 0.39e (in linear NThN^{2−}), of the same order as seen earlier [28,29]. For the metalloactinyls the typical values are smaller, 0.1e or less, as seen in Table 4. Is this trend related to orbital sizes

Table 5
Calculated bond lengths R_{AB} as compared with the sum of the triple-bond covalent radii [3]

System	Bond	R (calc)	r_A	r_B	$r_A + r_B$
AuThIr	Au–Th	285.9	123	136	259
	Th–Ir	224.0	136	107	243
PtThIr [−]	Pt–Th	248.3	110	136	246
	Th–Ir	227.6	136	107	243
OThIr [−]	O–Th	192.1	53	136	189
	Th–Ir	229.5	136	107	243

All values in pm.

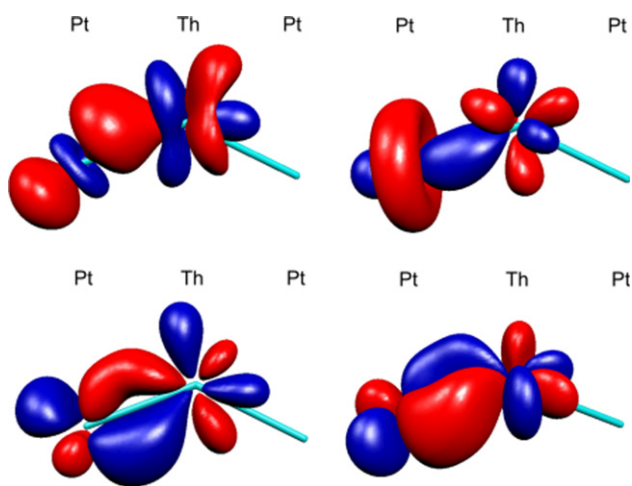


Fig. 2. The localized bonding orbitals for ThPt₂. The upper row shows a classical dσ–fσ bond (left) and a bond, partially involving the Pt 'doughnut' hybrid orbital (right), both at the same density level. The lower row shows the in-plane π bond (left) and the off-plane π bond (right). All four localized orbitals refer to the left-hand Pt–Th bond.

or orbital energies? From Desclaux' tables [30] one finds that for 6p(U), 5d(Pt) and 2p(O) of the neutral atoms, the radii $\langle r \rangle$ are 1.82, 1.66 and 1.24 au, while the spin-orbit-averaged orbital energies are 1.104, 0.415 and 0.616 au, respectively. This suggests that the larger hole for oxygen, as compared to platinum, is driven by its larger electronegativity. The 5d radius is not too large but the 5d binding energy is too small for effective interaction with the 6p(U).

On going from Th to Pa, a linear singlet ground state is obtained for PtPaPt⁺, with a bond-length of 234.1 pm. A linear triplet and a bent singlet (260.0 pm, 61.0°) lie 0.54 and 0.78 eV above the linear singlet, respectively. As noticed before [4], the isoelectronic PtUPt²⁺ goes triplet. The participation of 5f orbitals on Pa in bonding is larger than for Th, (NPA analysis s(0.61), p(0.00), d(0.36), f(2.00), 6p(5.90), Pa^{2.107}Pt^{−0.554}).

3.3. Vibrational frequencies

A sample of the calculated vibrational frequencies are given in Table 6. The ThO₂ results are compared with

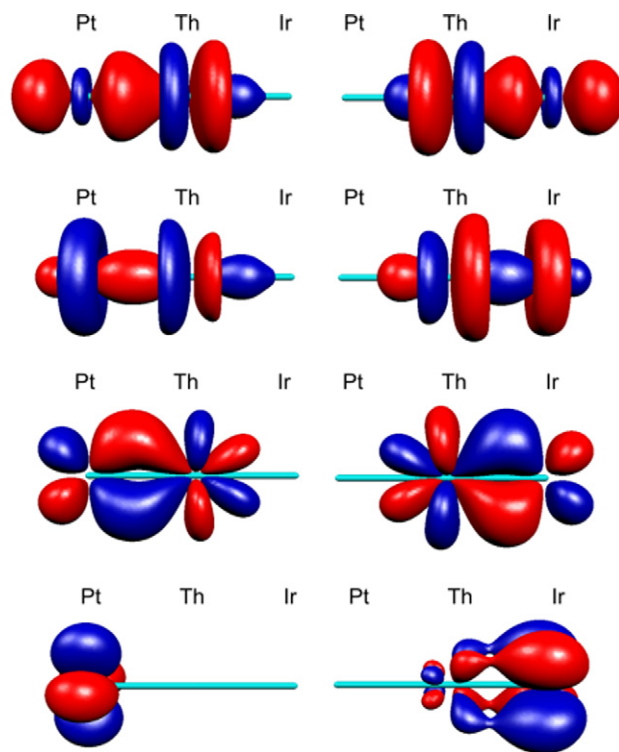


Fig. 3. The localized bonding orbitals for PtThIr[−]. The top row shows the classical fσ–dσ bonds. The second row shows, at the same density limit, the enhanced 'doughnut' σ orbitals (enlarged in Fig. 4). The third row shows the left and right π bonds. The bottom row shows the δ-ring at Pt and the, to some extent bonding, Th–Ir δ orbital.

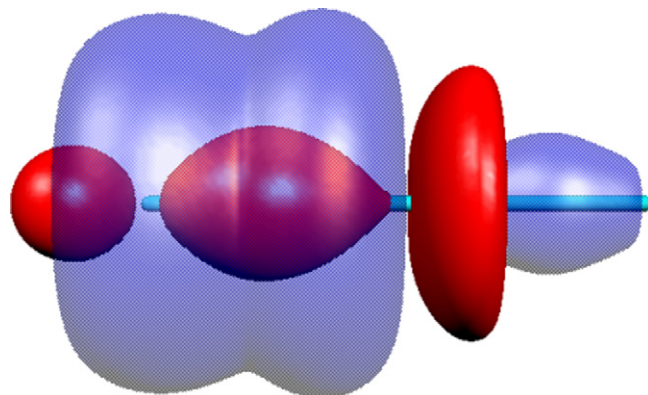


Fig. 4. The outer, bonding 'doughnut-σ' orbitals of PtThIr[−] with a lowered density limit.

the experimental ones, known since the work by Gabelnick et al. [16]. The small-core CCSD(T) results by Straka et al. [18] are also given. A comparison of OThO and OThPt suggests that the substitution of one O by Pt would increase the remaining Th–O stretching frequency by 17 cm^{−1}. That shift might be a way of observing the new species in matrix spectroscopy. The stretching vibrations in bimetalloactinyls lie in the range of 100–300 cm^{−1}.

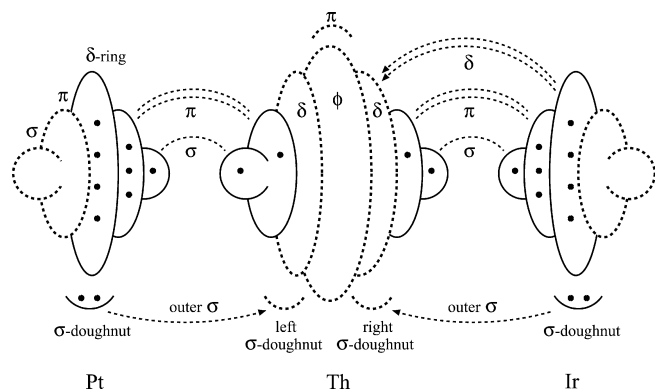


Fig. 5. A schematic description of the bonding in linear PtThIr⁻. Both Pt and Ir⁻ contribute 10e while Th contributes 4e, in total 24e. Both Pt and Ir have nine hybrid orbitals (left σ , left π , δ ring, doughnut σ , right π and right σ). Th has 16 orbitals (left $\sigma + \pi + \delta + \text{doughnut}$), (right $\sigma + \pi + \delta + \text{doughnut}$), a ϕ ring and an extra π . The predominant bonding comes from the left and right $\sigma^2\pi^4$ triple bonds, shown in Fig. 3. Moreover the outer, σ doughnut orbitals have some bonding character and so do the right-hand δ orbitals, with Ir-to-Th δ donation. The theoretical maximum bond order would be 4 and 6 for bonds of the left-hand and right-hand type, respectively.

Table 6
Harmonic frequencies (in cm⁻¹) for selected bent EThE' and EThM species in their singlet ground state

System	Bend	Stretch	Stretch	Comments
OThO	157	772 ^c	824 ^d	CCSD(T) [18] Exp. [16]
	166	748	802	
	–	735	787	
OThPt	81	209 ^a	841 ^b	
OThAu ⁺	87	150 ^a	939 ^b	
FThN	142	497 ^b	955 ^c	
FThIr	84	291 ^a	516 ^b	
NThAu	80	123 ^a	987 ^b	
FThO ⁺	123	603 ^b	930 ^c	
FThPt ⁺	89	252 ^a	617 ^b	
FThF ²⁺	105	700 ^c	725 ^d	
FThAu ²⁺	79	174 ^a	705 ^b	

^a Th–M stretching.

^b Th–E str.

^c Th–E' str.

^d Symm. str.

^e Asymm. str.

4. Conclusions

- (1) The idea of metalloactinyls can be extended to the case where the actinide is thorium or protactinium.
- (2) Like the known all-main-group EThE' species, most closed-shell MThE and MThM' systems are bent. The only exceptions are PtThIr⁻, NThIr²⁻ and the border-line cases OThIr⁻ and NThPt⁻.
- (3) A simple orbital-picture can be given to describe the bonding orbitals and main empty orbitals of these 16-orbital central elements.
- (4) Preliminary evidence is found for multiple bonding of order higher than three in certain cases. These involve δ -type donation from the 5d element to the actinide, and also a bonding combination of outer σ doughnut orbitals.

Acknowledgements

The stay of P.H. at Helsinki was supported by the European Commission through the EURATOM FP6 Integrated Project 'Fundamental Processes of Radionuclide Migration' (FUNMIG, www.funmig.com) and by COST Action D26, kindly organized by Professor Vladimir Malkin. M.S. was supported by a Marie Curie Intra-European Fellowships within the 6th European Community framework Program. This project was supported also by The Academy of Finland, projects 200903 and 206102, and belongs to the Finnish CoE in Computational Molecular Science.

References

- [1] P. Pykkö, M. Patzschke, J. Suurpere, Chem. Phys. Lett. 381 (2003) 45.
- [2] M. Patzschke, P. Pykkö, Chem. Commun. (2004) 1982.
- [3] P. Pykkö, S. Riedel, M. Patzschke, Chem. Eur. J. 11 (2005) 3511.
- [4] L. Gagliardi, P. Pykkö, Angew. Chem., Int. Ed. 43 (2004) 1573; L. Gagliardi, P. Pykkö, Angew. Chem. 116 (2004) 1599.
- [5] A.E. Reed, F. Weinhold, J. Chem. Phys. 83 (1985) 1736.
- [6] A.E. Reed, L.A. Curtiss, F. Weinhold, Chem. Rev. 88 (1988) 899.
- [7] M. Santos, J. Marçalo, A. Pires de Matos, J.K. Gibson, R.G. Haire, Eur. J. Inorg. Chem., DOI: 10.1002/ejic.200600562, electronically published 24 Jul 2006.
- [8] K.A. Gingerich, Chem. Phys. Lett. 23 (1973) 270.
- [9] K.A. Gingerich, S.K. Gupta, J. Chem. Phys. 69 (1978) 505.
- [10] R. Sternal, T.J. Marks, Organometallics 6 (1987) 2621.
- [11] J.M. Ritchey, A.J. Zozulin, D.A. Wroblewski, R.R. Ryan, H.J. Wasserman, D.C. Moody, R.T. Paine, J. Am. Chem. Soc. 107 (1985) 501.
- [12] P.J. Hay, R.R. Ryan, K.V. Salazar, D.A. Wroblewski, A.P. Sattelberger, J. Am. Chem. Soc. 108 (1986) 313.
- [13] L. Gagliardi, B.O. Roos, Nature 433 (2005) 848.
- [14] B.O. Roos, L. Gagliardi, Inorg. Chem. 45 (2006) 803.
- [15] M. Kaufman, J. Muentner, W. Klemperer, J. Chem. Phys. 47 (1967) 3365.
- [16] S.D. Gabelnick, G.T. Reedy, M.G. Chasanov, J. Chem. Phys. 60 (1974) 1167.
- [17] R.G. Denning, Gmelin Handbook of Inorganic Chemistry, U Supplement A6 (1983), p. 31.
- [18] M. Straka, K.G. Dyall, P. Pykkö, Theor. Chem. Acc. 106 (2001) 393.
- [19] K.G. Dyall, Mol. Phys. 96 (1999) 511.
- [20] H. Bolvin, U. Wahlgren, O. Gropen, C. Marsden, J. Phys. Chem. A 105 (2001) 10570.
- [21] P. Pykkö, L.J. Laakkonen, K. Tatsumi, Inorg. Chem. 28 (1989) 1801.
- [22] M.J. Frisch et al., GAUSSIAN 03, Revision C.02, Gaussian, Inc., Wallingford, CT, 2004.
- [23] D. Andrae, U. Häussermann, M. Dolg, H. Stoll, H. Preuss, Theor. Chim. Acta 77 (1990) 123.
- [24] W. Küchle, M. Dolg, H. Stoll, H. Preuss, J. Chem. Phys. 100 (1994) 7535.
- [25] F. Weigend, M. Häser, H. Patzelt, R. Ahlrichs, Chem. Phys. Lett. 294 (1998) 143.
- [26] A. Schäfer, C. Huber, R. Ahlrichs, J. Chem. Phys. 100 (1994) 5829.
- [27] P. Pykkö, J. Organomet. Chem., DOI: 10.1016/j.jorganchem.2006.01.064, electronically published 15 March 2006.
- [28] K. Tatsumi, R. Hoffmann, Inorg. Chem. 19 (1980) 2656.
- [29] S. Larsson, P. Pykkö, Chem. Phys. 101 (1986) 355.
- [30] J.P. Desclaux, At. Data Nucl. Data Tables 12 (1973) 311.